Int. J. Heat Mass Transfer. Vol. 10, pp. 1533–1558. Pergamon Press Ltd. 1967. Printed in Great Britain

HEAT TRANSFER TO NaK FLOWING THROUGH UNBAFFLED ROD BUNDLES*

SHELDON KALISH and ORRINGTON E. DWYER
Brookhaven National Laboratory, Upton, N.Y.

(*Received* 29 *March* 1967 *and in revised form* 15 *May* 1967)

Abstract—The paper presents the results of an extensive experimental study of heat transfer to NaK flowing through unbaffled rod bundles (or banks).

In-line flow results are reported on nine different test rods located in the center of a 19-rod bundle. They were obtained under conditions of fully established velocity and temperature profiles, and also under entrance-region conditions. The results on the first five test rods were in fairly good agreement with theoretical predictions and with earlier results obtained on mercury; but those on the last four fell low in the molecular-conduction (low-Péclet-number) regime. The lower the flow rate the lower the coefficients fell, indicating the presence of an interface resistance which was quite sensitive to the flow rate. It was concluded that the difficulty was due to less-than-perfect wetting of the heating surface, coupled with the presence of inert seal gas at the heating surface. The oxygen concentration in the NaK was at all times less than 25 ppm, which was far below the saturation level corresponding to the coldest part of the circulation loop.

Results were also obtained for 90°-cross and 45°-oblique flows through rod bundles, for the condition where only the test rod was heated and for that where all the rods were heated. Measurements were made at several rod locations in the bank, and both rod-average and circumferentially local heat-transfer coefficients were obtained.

The 90°-cross-flow results were in good agreement with previously published results on mercury, and with predictions based upon the theoretical correlation of Hsu [21]. In the low Péclet region, the all-rods-heated coefficients were appreciably higher than those for the condition where only the test rod was heated, but the difference decreased as the flow rate increased.

The 45°-oblique-flow coefficients, falling lower than Hsu's [26, 27] theoretical prediction, were 75 per cent of those for the 90°-cross-flow case.

The circumferential variation of the local normalized heat-transfer coefficient was found to be independent of flow rate, and the same for both 90°- and 45°-flow directions. Also, for both types of flow, the circumferential surface temperature profile was that of a simple cosine function.

On the basis of the results obtained in the study, supported by previous theoretical and experimental results, semi-empirical equations are proposed for predicting heat-transfer coefficients for both 90°- and 45°-cross flows for the condition where only the test rod is heated, and for that where all rods are heated.

NOMENCLATURE

a, empirical constant in equation (7); also major axis of ellipse [ft];
b, minor axis of ellipse [ft];
c, a constant defined by equation (22) [degF/ft];
C_p, specific heat [Btu/(lb_m degF)];
D, outside diameter of rods [ft];
D_e, $\dfrac{4(\text{total cross-sectional flow area})}{\text{total wetted perimeter}}$ [ft];
E, complete elliptical integral of the second kind, defined by equation (30);
h, in-line-flow heat-transfer coefficient for a rod in the interior of a bundle [Btu/(h ft^2 degF)];
h_c, "contact" heat-transfer coefficient [Btu/h ft^2 degF)];

* This work was performed under the auspices of the U.S. Atomic Energy Commission.

$h_{m.c.}$, in-line-flow heat-transfer coefficient for a rod in the interior of a bundle, in the molecular-conduction heat-transfer regime [Btu/(h ft^2 degF)];

h_θ, $= q_\theta/(t_{w,\theta} - t_b)$, local cross-flow heat-transfer coefficient at circumferential angle θ [Btu/(h ft^2 degF)];

$h_{0°}$, $= q_{0°}/(t_{w,0°} - t_b)$, local cross-flow heat-transfer coefficient at forward stagnation point [Btu/(h ft^2 degF)];

$h_{90°}$, $= q_{90°}/(t_{w,90°} - t_b)$, local cross-flow heat-transfer coefficient at $\theta = 90°$ [Btu/(h ft^2 degF)];

$\bar{h}_{w,\beta}$, $= \bar{q}/\bar{t}_{w,\beta}$, rod-average heat-transfer coefficient in cross flow [Btu/(h ft^2 degF)];

$\bar{h}_{w,45°}$, $= \bar{q}/\bar{t}_{w,45°}$, rod-average heat-transfer coefficient in 45°-cross flow [Btu/(h ft^2 degF)];

$\bar{h}_{w,90°}$, $= \bar{q}/\bar{t}_{w,90°}$, rod-average heat-transfer coefficient in 90°-cross flow [Btu/(h ft^2 degF)];

k, molecular thermal conductivity [Btu/(h ft degF)];

k_c, thermal conductivity of copper [Btu/(h ft degF)];

k_e, eddy thermal conductivity [Btu/(h ft degF)];

L_f, distance along test element from flow inlet [ft];

L_H, total heated length of test element [ft];

L_h, distance along heated length of test element from direction of flow inlet [ft];

Nu, $= hD_e/k$, in-line-flow Nusselt number for a rod in the interior of a bundle [dimensionless];

$Nu_{m.c.}$, $= h_{m.c.}D_e/k$, in-line-flow Nusselt number for a rod in the interior of a bundle, in the molecular-conduction heat-transfer regime [dimensionless];

$[Nu]_\beta$, $= \bar{h}_{w,\beta}D/k$, Nusselt number for cross flow [dimensionless];

$[Nu]_{45°}$, $= \bar{h}_{w,45°}D/k$, Nusselt number for 45°-cross flow [dimensionless];

$[Nu]_{90°}$, $= \bar{h}_{w,90°}D/k$, Nusselt number for 90°-cross flow [dimensionless];

P, pitch, distance between rod centers [ft];

Pe, $= (D_e v_a \rho C_p)/k$, Péclet number for in-line flow [dimensionless];

$[Pe]_{v,\text{free}}$, $= (Dv_{\text{free}}\rho C_p)/k$, Péclet number based on v_{free} in cross flow [dimensionless];

$[Pe]_{v,\max}$, $= (Dv_{\max}\rho C_p)/k$, Péclet number based on $v_{\max}$ in cross flow [dimensionless];

Pr, $= C_p\mu/k$, Prandtl number [dimensionless];

q_θ, local heat flux at angle θ on the circumference of a rod [Btu/(h ft^2)];

$q_{0°}$, local heat flux at forward stagnation point on the circumference of a rod [Btu/(h ft^2)];

$q_{90°}$, local heat flux at $\theta = 90°$ on the circumference of a rod [Btu/h ft^2)];

$q)_{r=r_1}$, heat flux at r_1 [Btu/(h ft^2)];

$\bar{q}$, rod-average value of q in cross flow [Btu/(h ft^2)];

r, radial distance through rod sheath [ft];

r_1, inside radius of rod sheath [ft];

Re, $= (D_e v_a \rho)/\mu$, in-line-flow Reynolds number [dimensionless];

t, sheath temperature at radius r [°F];

t_b, bulk temperature of flowing NaK at same distance through bundle (or bank) as point at which t_w is measured [°F];

t_w, surface temperature of rod in in-line flow [°F];

$\bar{t}_{w,\beta}$, average circumferential surface temperature of rod in cross flow at any angle β [°F];

$\bar{t}_{w,45°}$, average circumferential surface temperature of rod in 45°-cross flow [°F];

$\bar{t}_{w,90°}$, average circumferential surface temperature of rod in 90°-cross flow [°F];
$t_{w,\theta}$, local surface temperature of rod at circumferential angle θ [°F];
$t_{w,0°}$, local surface temperature of rod at forward stagnation point [°F];
$t_{w,90°}$, local surface temperature of rod at circumferential angle of 90° [°F];
v_a, average linear velocity of NaK through bundle in in-line flow [ft/h];
v_{free}, average cross-flow stream velocity without presence of rods [ft/h];
v_{max}, cross-flow velocity through rod bank, based on the minimum flow area [ft/h];
W, electrical energy delivered to test element [W];
$\bar{x}$, distance along the outside diameter of the tube measured from the forward stagnation point [ft].

Greek symbols

β, angle between axes of rods and the direction of flow (see Fig. 18) [degrees];
ϵ_H, $= k_e/\rho C_p$, eddy diffusivity of heat [ft^2/h];
ϵ_M, eddy diffusivity for momentum transfer [ft^2/h];
θ, circumferential angle measured from the front stagnation point (see Fig. 14) [degrees];
μ, dynamic viscosity [$lb_m/(ft\,h)$];
ν, kinematic viscosity [ft^2/h];
ρ, density [lb_m/ft^3];
σ, empirical constant defined by equation (8);
Φ, hydrodynamic potential function;
ϕ, $= \Phi/v_{free}$ unit hydrodynamic potential function;
ϕ_1, unit velocity potential at the rear stagnation point of a rod;
$\bar{\psi}$, effective average value of ratio ϵ_H/ϵ_M.

1. INTRODUCTION

This paper presents experimental heat-transfer results obtained for the flow of NaK through unbaffled rod bundles, where the direction of flow with respect to the rods was of three types: in-line, or parallel, flow; 90°-cross, or perpendicular, flow; and 45°-cross, or oblique, flow. Such information is pertinent to the thermal design of cores and heat exchangers for liquid–metal cooled nuclear power reactors. The experiments were the first of their type carried out in the U.S. with an alkali metal.

As far as the in-line-flow experiments are concerned, previous investigations [1, 2, 3] of this type were carried out at Brookhaven with mercury, and the main purpose of the present experiments was to see if the alkali–metal results would agree with those obtained on mercury.

The 90°-cross-flow investigation was carried out for a similar reason. There had been two previous experimental studies [4, 5] of this type carried out at Brookhaven, with mercury. But, whereas in those studies only the test rod in the bundle was heated, in the present one, data were taken first with only the test rod heated and then with all rods heated, for comparison.

The 45°-cross-flow study was done because of its importance in the design of liquid–metal shell-and-tube heat exchangers. On the shell side of such exchangers, the liquid metal flows across the tube bundle in all directions from parallel to perpendicular. There are no experimental results reported in the literature for the 45°-cross-flow case.

All of the heater rods used in this study were the standard type of electrical-resistance heaters, consisting of a central Nichrome heating coil, electrically insulated from the outer sheath by compressed MgO. The rate of heat generation in the Nichrome coil was uniform with length, and the coil was centrally located in the heater assembly. The in-line experiments were carried out under the condition of uniform heat flux in all directions. However, due to circumferential flow in the copper sheaths, the heat flux in the cross-flow experiments was not uniform in the circumferential direction.

Because this is a long paper, the following outline of it is given for the convenience of the reader.

2. LOOP OPERATION

The work was carried out in a loop facility especially designed for single-phase alkali-metal heat-transfer studies at temperatures up to 900°F. The circuit was built of $2\frac{1}{2}$-in schedule 40 304 stainless steel pipe and was of all-welded construction. NaK recirculation rates of up to 150 g/m against a 42-ft head were obtainable with an electrodynamic pump.

Besides the test section, the principal components of the loop were two flowmeters, a surge tank, a dump tank, and a finned air-cooled heat exchanger. The surge tank, located at the top of the loop, contained argon seal gas and provided a 3·5 ft^2 NaK–argon interface. Each cylinder of argon was analyzed for O_2 and H_2O before use, and only cylinders showing less than 20 ppm of combined O_2 and H_2O were used. About 5 per cent of the flowing stream passed through the surge tank. The finned air cooler removed the energy added to the flowing NaK in the test section and by the pump.

2.1. *Oxygen control*

The loop was charged by pressurizing the dump tank while its contents were at room temperature, the NaK flowing through a 10-μ micrometallic filter. This meant that the oxygen content of the NaK in the loop could not be above that corresponding to the saturation value at room temperature. To reduce the oxygen content below that, the contents of the loop were circulated at a rate of about 2 g/m through the hot trap which was filled with titanium chips and held at a temperature of 1400°F. A standard plugging-valve indicator was used to measure the oxygen concentration and at no time during the course of the investigation was the plugging temperature in excess of 250°F, which corresponds to an oxygen content of about 25 ppm. This meant that the oxygen content of the NaK circulating in the loop was at all points and at all times far below saturation levels.

2.2. *Flow rates*

These were measured with venturi and electromagnetic flowmeters, both of which were previously calibrated. The latter had a wider operating range. In the flow range where both meters were applicable, they agreed to within 2 per cent.

* This portion of the study was presented at the ASME–AIChE Heat Transfer Conference as Paper No. 65-HT-11, Los Angeles, Calif., August 8–11 (1965).

Table 1. Rod bundle measurements, and scope of experimental studies

Bundle (or bank) measurements	In-line test section	90°-cross-flow test section	45°-cross-flow test section
1. Number of rods in bundle	19	63 (including unheated "half-rods" at wall)	63 (including unheated "half-rods" at wall)
2. Outside diameter of rods [in]	0·500	0·500	0·500
3. Shell cross-section	4·654-in-I.D. circle	7-in high × 6·125-in wide	7-in high × 6·125-in wide
4. Lattice geometry	equilatereal triangular	equilateral triangular	equilateral triangular
5. Pitch-to-diameter ratio	1·75	1·75	1·75
6. Distance between end plates [in]	71·5	7·00	7·00
7. Length of rods between plates	71·5	7·00	9·90
8. Length of rods between flow nozzles [in]	62·0	—	—
9. Total heated length [in]	44·7	6·75	9·65
10. Equivalent diameter [ft]	0·100	—	—
Scope of study			
1. Prandtl number range	0·013–0·021	0·017	0·015
2. Reynolds number range	12000–92000	2350–20600	2600–23000
3. Péclet number range	250–1200 ($D_e v_a \rho C_p/k$)	40–230 ($D v_{max} \rho C_p/k$)	40–350 ($D v_{max} \rho C_p/k$)
4. L_f/D_e range	12·4–42·4	—	—
5. Heat flux [Btu/(h ft^2)]	18000–30000	35000–60000	30000–40000
6. Temperature range [°F]	275–650	≈400	≈450
7. Flow direction	vertically upward	horizontal	horizontal

3. IN-LINE FLOW

3.1. *Test section*

This consisted of a nineteen-rod bundle of 0·500-in rods having an equilateral triangular spacing. The remaining statistics of the rod bundle are given in Table 1.

All nineteen rods were electrically heated with alternating current at voltages up to 220. The central rod was the only one on which data were taken. It is known [6] that the thermal behavior of such a rod would be the same as one in the interior of a much larger bundle, i.e. no interfering effects from the periphery of the bundle. The designs of the test element and other rods were essentially the same as those described in [2]. The surface temperatures of the test elements were measured by means of copper-sheathed Chromel–Alumel thermocouples imbedded very slightly below the surface, as described in [2]. Construction details of the ten different test elements used in the study are summarized in Table 2.

Table 2. Test element details

Test element	0·100-in sheath	Underplate	Overplate	Thermocouple locations, L_f/D_e
1	copper	0·0008-in Ni	0·0001-in Cr	27·4 (1), 31·1 (2), 34·8 (2), 38·6 (2), 43·3 (2)
2	copper	—	0·0008-in Ni	all at 38·6
3	copper	—	0·0008-in Ni	all at 38·6
5	copper	—	0·0008-in Ni	all at 38·6
6	copper	—	0·0008-in Ni	12·4, 16·1, 19·9, 23·6, 27·4, 31·2, 34·9, 38·6, 42·4
7	copper	—	0·0008-in Ni	all at 38·6
8	copper	—	0·0008-in Ni	12·4, 16·1, 19·9, 23·6, 27·4, 31·2, 34·9, 38·6, 42·4
9	nickel	0·0008-in Ni	0·0001-in Cu*	all at 38·6
10	copper	—	0·0008-in Ni	all at 38·6

* The copper overplate on this element was tinned with mercury just prior to insertion into test section.

To prevent bowing by thermal expansion, the rods were free to slip through a bottom guide sheet. The lower ends of the rods were electrically grounded in a pool of NaK at the bottom of the test section. This was accomplished by welding a cap to the sheath and lower terminal of each heater. The rods were cleaned with butanol and wiped dry just prior to their insertion in the test section. They were within 0·003 in of being perfectly straight.

3.2. *Instrumentation*

Bulk temperatures of the NaK entering and leaving the test section were measured by thermocouples grounded in thermowells. There was one in each of the two branch lines leading to and the two branch lines leading from, the test section. In addition there were three in the main line leading to, and three in the main line leading from, the test section. These thermocouples, along with the nine on the test element, were checked against each other while the NaK was isothermally circulated in the loop at a high flow rate. The average of the bulk-temperature thermocouples was chosen as a reference, against which all the individual thermocouples were calibrated. This checking of the thermocouples was done periodically with each test element.

It was demonstrated that there was no e.m.f. pickup by the thermocouples as a result of any magnetic fields produced by the alternating current.

The high-precision K-wattmeters which were used for measuring the power input to the test elements, to the other eighteen rods, and to the shell heaters were all calibrated before, and frequently during, use.

3.3. *Experimental procedure*

Since the equivalent diameter of the test section assembly was the same as the nominal value for the bundle, the average velocity of the NaK in the space between the bundle and the shell was the same as that between the rods. To heat the NaK flowing between the bundle and the shell to the same extent as that flowing between the rods, the power to the shell heaters was carefully controlled. Those heaters were embedded in Thermon heat-transfer cement under a 4-in layer of high temperature insulation.

In a given run, the power required on the shell heaters depended on the power level of the internal heaters and on the heat loss from the test section. Prior to making a run, the heat balance could be closely estimated and the proper settings determined for the shell heaters. The estimated power requirements were generally within 5 per cent of the correct values. It was found that the shell power level had an effect on the measured heat-transfer coefficient. For example, an excess of 5 per cent power on the shell increased the coefficient by about 3 per cent; and this was independent of the Péclet number. This is in general agreement with results obtained previously at Brookhaven with mercury [2].

Steady-state conditions were carefully established before final data were taken. This required from 1 to 5 h, depending upon the thermal conditions of the loop at the time a run was started.

The physical properties of NaK-44 used in the calculations were taken from [7].

3.4. *Theoretical considerations*

There have been several analytical studies [2, 8–11] carried out in recent years for the case of heat transfer to liquid metals flowing in-line through unbaffled rod bundles. All of them were based on the conditions of uniform heat flux and fully developed flow. Four of them assumed an annulus model, (i.e. the coolant flow area associated with each rod is bounded by a circle instead of a hexagon) which is good down to a P/D ratio of about 1·4. In the P/D range of 1·4–1·75—that considered in the present study—the heat-transfer correlations based upon these studies are in rather good agreement. Their differences result, for the most part, from the methods used in determining the radial velocity-profiles in the flowing liquid metal.

Nimmo and Dwyer [3] showed that the two correlations of [2] agreed well with heat-transfer coefficients obtained with mercury. One correlation was for the molecular-conduction regime (at low Péclet numbers). It is

$$Nu_{m.c.} = -2{\cdot}79 + 3{\cdot}97\,(P/D) + 1{\cdot}025\,(P/D)^2 + 3{\cdot}12 \log_{10} Re - 0{\cdot}265\,(\log_{10} Re)^2. \quad (1)$$

The other was for the combined molecular-conduction/eddy-conduction regime (at medium and high Péclet numbers). It is

$$Nu = \alpha + \beta[\psi Pe]^{\gamma} \quad (2)$$

where

$$\alpha = 6{\cdot}66 + 3{\cdot}126\,(P/D) + 1{\cdot}184\,(P/D)^2$$
$$\beta = 0{\cdot}0155$$
$$\gamma = 0{\cdot}86.$$

They evaluated the quantity $\bar{\psi}(= \epsilon_H/\epsilon_M)$ by the empirical equation

$$\bar{\psi} = 1 - \frac{1{\cdot}82}{Pr(\epsilon_M/\nu)^{1{\cdot}4}_{\max}} \quad (3)$$

proposed earlier by Dwyer [12].

Curve A–A in Fig. 1 represents equation (2), when $\bar{\psi}$ is taken as unity; curve B–B represents equation (2), with $\bar{\psi}$ evaluated by means of equation (3); and curve C–C represents equation (1). The combination curve C–B–B therefore represents the predicted Nu–Pe relationship in the present case.

3.5. *Experimental results*

The results obtained on test elements 1, 2, 3, 5, and 6 are shown together in Fig. 1. Taken together, the data points show appreciable scatter. The average deviation from the dashed lines is ± 8 per cent; but, for a single element, the average deviation was very much less. The results from element 4 were omitted from Fig. 1 because they fell low and showed a large circumferential temperature variation, which was later found to be due to the fact that the internal Nichrome heating wire was considerably off-center.

The coefficients were calculated by the equation

$$h = \frac{3{\cdot}413\,W}{\pi D L_H(t_w - t_b)}. \quad (4)$$

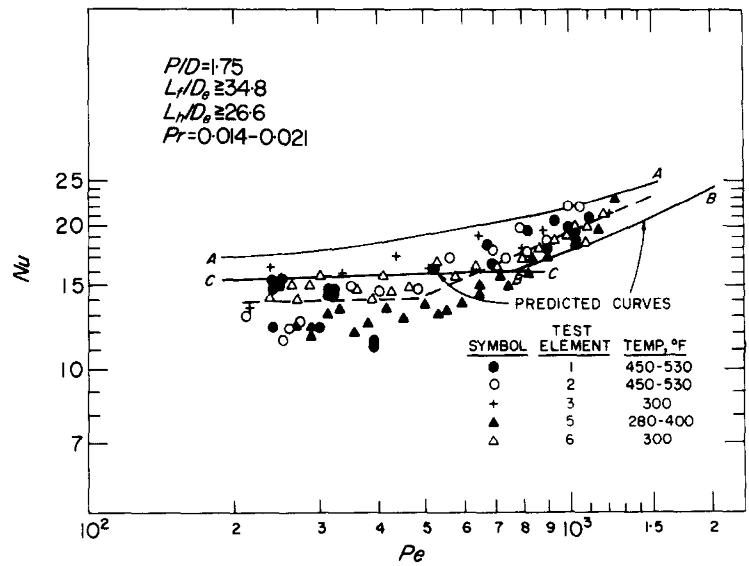

FIG. 1. Heat transfer to NaK flowing in-line through an unbaffled rod bundle under conditions of uniform heat flux and fully established flow. The experimental results are represented by dashed "dog-leg" curve.

It is seen that both the experimental and theoretical curves show the characteristic "dog-leg" shape predicted earlier by Dwyer [12] and observed by Maresca and Dwyer [2] and Nimmo and Dwyer [3] with mercury. In the lower half of the Péclet number range studied, the experimental curve falls about 10 per cent below the predicted curve, whereas in the upper half it falls about 10 per cent above it. As a result, the "knee" of the experimental curve occurs at a Péclet number of 500 instead of the predicted 700. Thus, up to a Péclet number of 500, or, in other words, up to a Reynolds number of about 25000, the heat-transfer coefficient is essentially constant, indicating the absence of eddy transport in the heat-transfer mechanism.

It is interesting to compare the results in Fig. 1 with those recently [2, 3] published for heat transfer to mercury under similar conditions. At the lower end of the Péclet range, the results in Fig. 1 agree very well with those in [2] while at the higher end they fall about 10 per cent higher. At the lower end of the Péclet range, the results in Fig. 1 fall about 15 per cent below those in [3], while at the higher end they are in good agreement. Here, the lower and higher ends of the Péclet range represent the molecular-conduction and molecular-plus-eddy-conduction regimes, respectively.

In general, it can be concluded that the present NaK results and the earlier mercury ones are in moderately good agreement. The slight differences that do exist appear to be within the expected variations in results obtained with liquid metals on different experimental rigs. Moreover, the differences between the present NaK results and either set of mercury results [2, 3] is no greater than the differences between the mercury results themselves.

There appears to be a strong tendency for both the NaK and mercury Nusselt numbers in the molecular-conduction regime to fall about 10 per cent below the calculated curve. It is suspected that this may be due to the method of determining t_b. At low flow rates, there is a relatively large temperature rise through the test bundle, and a small consistent error in determining t_b would have a relatively large effect on the temperature drop, $\bar{t}_w - t_b$. Owing to the fact that these temperature drops are small, it is estimated that only about a 1 degF error in t_b could account for the discrepancy between the predicted and experimental curves in the molecular-conduction regime.

Some test elements had the nine surface thermocouples located at the same axial location and 40° apart on the periphery. Others had them strung out along their lengths. In the former case, the surface temperatures were averaged; in the latter, only one temperature reading was available, but Nu was taken from a smooth curve drawn through the points on a Nu vs. L plot. When the nine thermocouples were located at the same axial location, the average deviation of the nine temperatures from the mean was only about 5–10 per cent of the ($\bar{t}_w - t_b$) difference.

The bulk temperature t_b was calculated from measured values of the inlet and outlet stream temperatures, assuming that the heat fluxes were axially uniform.

Test element 1 had a chromium electroplate, while 2, 3, 5, and 6 had nickel electroplates. There was no apparent difference in the heat-transfer characteristics between the chromium and nickel surfaces.

The results shown in Fig. 1 were taken over the temperature range 280–530°F. There was no observable effect of temperature.

3.5.1. *Entrance effects.* Test element 6, as described in Table 2, had its nine thermocouples strung out along its length. The results obtained from these thermocouples are shown in Fig. 2. It is seen that an entrance length of thirty-five equivalent diameters was required to establish fully developed heat-transfer coefficients. It required this length to develop the velocity profiles. The lengths required to develop temperature profiles (with fully developed velocity profiles) are only about one-third those required to establish fully developed velocity profiles [13].

Over the five-fold range of Reynolds number which was employed, there was no discernible effect of flow rate on the value of the L_f/D_e ratio required to establish fully developed flow. For the same flow channel, the value of this ratio depends upon the type of inlet-flow connection. In the present case, it was designed to minimize inlet turbulence.

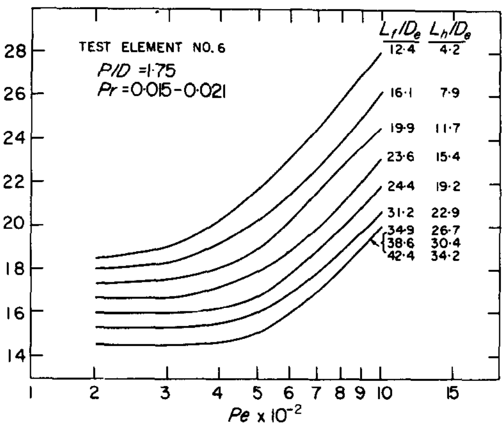

FIG. 2. Heat transfer to NaK flowing in-line through an unbaffled rod bundle, under condition of uniform heat flux, showing entrance-region effects. (The test results from element 6 were very representative.)

The results shown in Fig. 2 are consistent with those obtained by Maresca and Dwyer [2] for mercury flowing through a similar rod bundle. There, the size and spacing of the rods were the same as in the present study, but the bundle had only thirteen rods. This would have required a shorter L_f/D_e ratio to establish fully developed flow, and they reported a value of 27·3. The value of the L_f/D_e ratio to establish fully developed flow is, of course, not a sharply defined point. This also could account for some of the discrepancy between the two studies.

The data points are omitted in Fig. 2 to avoid cluttering up the plot. The average deviation of the points from the curves shown was about ± 3 per cent.

3.5.2. *Drop in coefficients.* About half way through the study, the heat-transfer coefficients at the lower Péclet numbers suddenly fell unexpectedly low. Those obtained with element 7 turned out to be very different from those obtained with the previous elements. They gave essentially a straight line relationship on a *Nu* vs. *Pe* plot, which resulted in the Nusselt numbers at the low end of the Péclet range being well below the laminar-flow value.

The results on elements 8, 9, and 10 were in general agreement with those on 7. They are all shown in Fig. 3. Several months were spent in an exhaustive attempt to find an explanation for the apparent anomaly, without complete success. It was proved that the difficulty was not due to any of the following: (a) bowing of rods, (b) change in general purity of the NaK, (c) change in oxide content of the NaK, (d) malfunctioning of thermocouples, (e) malfunctioning of instruments, (f) oxidation of the surface metal, and (g) axial heat conduction.

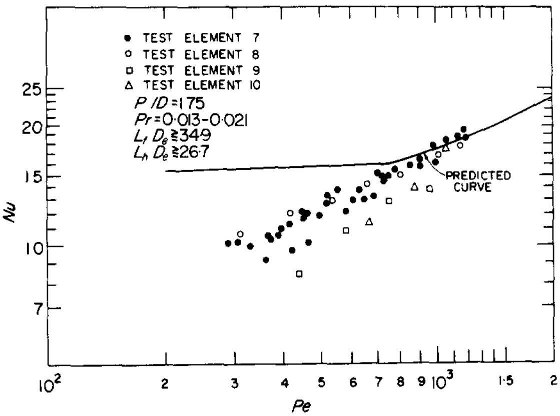

FIG. 3. Heat transfer to NaK flowing in-line through an unbaffled rod bundle, under conditions of uniform heat flux and fully established flow. These results are low in the molecular-conduction regime, due to a flow-dependent thermal conductance at the wall.

The results in Fig. 3 show that, whatever was causing the low results, it was greatly affected by flow rate, for at the high end of the Péclet range its influence was negligible. A best-fit line was drawn through the points in Fig. 3 and then used to calculate "contact" heat-transfer coefficients. The results are plotted in Fig. 4 as reciprocal contact Nusselt number vs. Reynolds number for an average Prandtl number of 0·017. It is seen that the "contact" resistance decreased rapidly with flow rate, becoming negligible at $Re = 70000$.

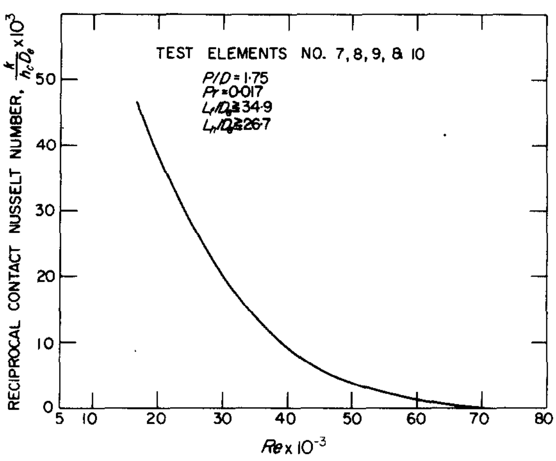

FIG. 4. Effect of flow rate on thermal "contact" resistance at surface of test element.

Subbotin and co-workers [14, 15] have obtained curves similar to that in Fig. 4 for mercury flowing through steel tubes, except that the thermal contact resistances which they measured were considerably higher than those found here. They obtained their contact resistances by measuring the wall temperature and the radial temperature distribution across the flowing stream.

The curve in Fig. 4 suggests some kind of added resistance near the wall in the laminar sublayer, or between the heating surface and laminar sublayer. It was found that this resistance was decreased by doing the following, in addition to increasing the flow rate: (a) increasing the temperature, (b) brushing the element with a stainless steel wire brush while submerged in the NaK, and (c) decreasing the argon (seal gas) pressure. This is demonstrated graphically in Fig. 5.

These findings led to the conclusion that the low results with elements 7 through 10 were caused by a combination of gas and less-than-perfect wetting. In the case of mercury, it is easy to get completely "wetted" or completely "unwetted" heat-transfer surfaces, and in either case the coefficients are not significantly different [1, 2, 3], as long as the mercury is free from particulate matter. However, in the case of alkali metals, it appears that, more often than not, the heat-transfer surfaces are less than completely wetted. Under this condition, gas can collect at the heat-transfer surface.

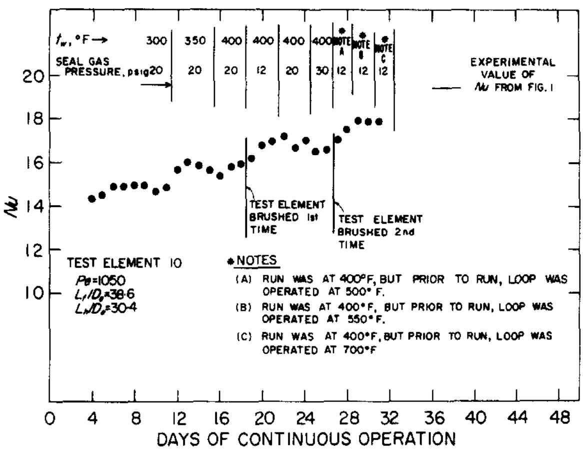

FIG. 5. A time-history plot of heat-transfer data taken on element 10, showing how various actions affected the Nusselt number.

Element 8 had its thermocouples strung out along its length, and it was observed that at low values of L_f/D_e the coefficients agreed rather closely with those from elements 1 and 6, whereas under conditions of fully established flow they fell much lower than those from 1 and 6. This indicates that under conditions of high wall shear stress, as exists in high flow rates, the adverse effect of gas collection at the heating surface is greatly mitigated.

The evidence therefore strongly suggests that the low coefficients obtained in the molecular-conduction regime, as illustrated in Fig. 3, were due to the coexistence of two conditions, i.e. the presence of gas at the walls and less-than-perfect wetting. This conclusion is consistent with the fact that, for a constant flow rate, an increase in seal gas pressure depressed the heat-transfer coefficient, as illustrated in Fig. 5.

The solubility of noble gases in alkali metals increases with temperature, and the surge tank in the loop was located directly after the test section which meant that its temperature was the highest in the circuit. This further meant that, in all probability, the NaK leaving the surge tank contained more argon than it could hold at the lowest temperature in the circuit, which was at the inlet to the test section. The excess argon could collect at the heating surface, either adsorbed on the wall or entrained in the form of very fine bubbles in the laminar sublayer. It is thus apparent that the greater the temperature rise in the test section, the greater the gas precipitation problem would be. This is obvious from Fig. 3 where low Péclet numbers mean low flow rates and therefore large temperature rises across the test section. In general, the temperature difference ($t_w - t_b$) was only about 30 per cent of the temperature rise across the test section, which meant that the laminar layer near the wall was not hot enough to dissolve the excess argon in the test section.

The big question remaining is this: Why did not the gas problem arise during the period in which the first six test elements were used? We have no satisfactory answer for this troublesome question.

Encountering very low coefficients in the low Péclet range for in-line flow through rod bundles is nothing new. This has been observed by Subbotin, Ushakov, and Kirillov [16] and by Borishansky and Firsova [17, 18]. The first of these teams measured rod-average heat-transfer coefficients for in-line turbulent flow of mercury through heated rod bundles having P/D ratios ranging from 1·1 to 1·5. The rods have stainless-steel sheaths with imbedded thermocouples. The second team carried out a similar study with Na where the heater sheaths were made of copper.

Results from both of these studies are compared with theoretical predictions in Figs. 26 and 31 of [19]. It will be seen in both of these figures that, in the low Péclet range, the Nusselt numbers fall far below the constant laminar-flow line, which is a theoretical impossibility for a clean, gas-free system.

In other words, both of these sets of results apparently suffer from a similar difficulty as those presented in Fig. 3—an additive resistance at the wall which is greatly dependent on the flow rate.

We conclude that the anomalous heat-transfer results reported, and referred to, above have nothing to do with any inherent thermal characteristic of liquid metals, but is simply due to poor thermal conductance at the heating surface caused by either gas or oxides, or both. In the present study, however, it was definitely shown that oxides or other impurities were not the cause of the low heat-transfer coefficients. At one point, the NaK was completely replaced with a fresh charge, but the coefficients remained unchanged.

4. 90°-CROSS FLOW

4.1. *Theoretical considerations*

In 1958, Cess and Grosh [20] published the results of an analytical study in which they developed theoretical equations for estimating 90°-cross-flow heat-transfer coefficients for liquid metals flowing through tube banks or rod bundles. They made the following assumptions:

1. Heat transfer occurs under steady-state, two dimensional flow conditions,
2. Eddy thermal transport is negligible compared to molecular conduction,
3. Physical properties are independent of temperature,
4. Contact resistance at liquid–solid interface is negligible,
5. Flow is inviscid and irrotational,

6. The hydrodynamic potential distribution on the surface of a tube is

$$\phi = \phi_1 \frac{\bar{x}}{D} \tag{5}$$

where

$\phi = \Phi/V$ = unit hydrodynamic potential function,
Φ = hydrodynamic potential function,
V = uniform free stream velocity, i.e. without presence of tubes,
$\bar{x}$ = distance along the outside diameter of a tube measured from the forward stagnation point,
D = outside diameter of tubes.
ϕ_1 = unit hydrodynamic potential at the near stagnation point on a rod.

7. Interaction between the thermal boundary layers of the tubes in a tube bank is negligible.

Assumptions 2 and 5 are admissible, particularly for liquid metals, as long as the flow rates are not high. Thus, equation (6) below will predict low coefficients at high Péclet numbers, as we shall see later. Assumption 7 is less apt to be true for liquid metals than for ordinary fluids where the thermal boundary layers are thin. This assumption implies that the heat-transfer coefficient is the same whether one or all rods in the bundle are transferring heat to the flowing stream.

On the basis of their study, Cess and Grosh proposed four equations each for an arbitrary temperature or heat flux distribution around the surface of the tube. For the case of a cosine surface-temperature distribution, their final equation was

$$[Nu]_{90^\circ} = 0{\cdot}718\left(\frac{\phi_1}{D}\right)^{\frac{1}{2}}[Pe]_{v,\,\mathrm{free}}\left(1 + \frac{\sigma}{3}\right) \tag{6}$$

where the circumferential surface temperature variation is represented by the equations

$$t_{w,\theta} - t_b = (\bar{t}_{w,\,90^\circ} - t_b) - a\cos\theta \tag{7}$$

and

$$\sigma = \frac{a}{\bar{t}_{w,\,90^\circ} - t_b}. \tag{8}$$

The Péclet number in equation (6) is defined by the equation

$$[Pe]_{v,\,\mathrm{free}} = \frac{Dv_{\mathrm{free}}\,\rho C_p}{k}. \tag{9}$$

Cess and Grosh used a conducting-sheet analog to determine values of ϕ_1/D for different geometrical arrangements of the tubes. One of the drawbacks of equation (6) is that σ must be determined from experimental results. In Fig. 6 it is compared with experimental results obtained in the present study where σ was obtained from the same experimental results and given by the expression

$$\sigma = 0{\cdot}087\,[Pe]_{v,\max}^{0{\cdot}278}. \tag{10}$$

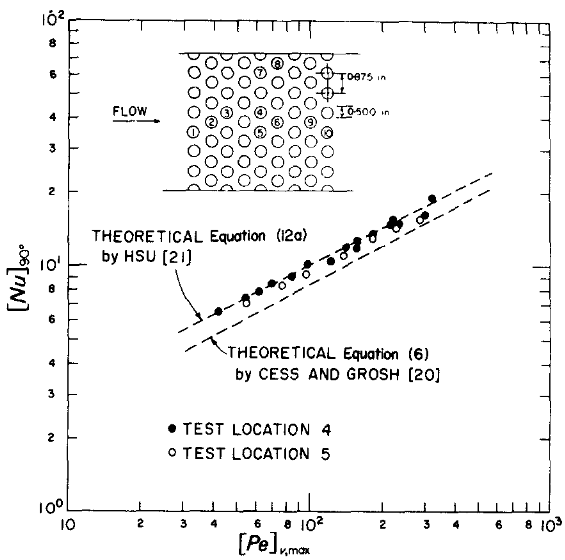

FIG. 6. Comparison between experimental results and theoretical predictions for heat transfer for 90°-cross flow of NaK through a staggered rod bank. Nusselt numbers are for test rods located in the interior of the bank, with only the test rod heated.

As we shall see later, the circumferential surface temperature distributions observed in the present study could be rather closely represented by equation (7).

In 1964, Hsu [21] published the results of another study similar to that of Cess and Grosh.

He employed all the assumptions made by Cess and Grosh but he did two things differently. First, he evaluated the variable quantity ϕ_1/D by means of mathematical functions originally developed by Howland and McMullen [22]; and secondly, he expressed the surface temperature variation by the equation

$$t_{w,\theta} - t_{w,0^\circ} = (t_{w,90^\circ} - t_{w,0^\circ})(1 - \cos\theta) \tag{11}$$

which he found to represent rather well the data of Hoe *et al.* [4] for mercury flowing through a staggered rod bank.

Hsu presented tabulated values of the ϕ_1/D ratio, which is a unique function of the spatial arrangement of the rods, for both square and equilateral patterns. They agreed quite closely with those obtained by Cess and Grosh, being never more than 5 per cent off. His final correlating equations were

$$[Nu]_{90^\circ} = 0{\cdot}958\,(\phi_1/D)^{\frac{1}{2}}\,[Pe]^{\frac{1}{2}}_{v,\text{free}} \tag{12}$$

for a simple cosine surface temperature distribution around the rod, and

$$[Nu]_{90^\circ} = 0{\cdot}810\,(\phi_1/D)^{\frac{1}{2}}\,[Pe]^{\frac{1}{2}}_{v,\text{free}} \tag{13}$$

for the uniform-heat-flux case. It is seen that the coefficients for the first case are about 18 per cent larger than those for the second. It is further seen, by comparing the lines in Fig. 6, that equation (6) gave coefficients which were about 15 per cent lower than those by equation (12). The difference between these two equations is partly due to the different expressions for the circumferential surface temperature variation, i.e. equation (7) vs. (11). The abscissa in Fig. 7 is $[Pe]_{v,\max}$, which is related to $[Pe]_{v,\text{free}}$ by equation

$$[Pe]_{v,\max} = \left(\frac{P}{P - D}\right)[Pe]_{v,\text{free}}, \tag{14}$$

for the present geometry, shown in Fig. 7. Thus, in this case we can re-write equations (12) and (13) as

$$[Nu]_{90^\circ} = 0{\cdot}958\,(\phi_1/D)^{\frac{1}{2}}\left(\frac{P - D}{P}\right)^{\frac{1}{2}}[Pe]^{\frac{1}{2}}_{v,\max} \tag{12a}$$

and

$$[Nu]_{90^\circ} = 0{\cdot}810\,(\phi_1/D)^{\frac{1}{2}}\left(\frac{P - D}{P}\right)^{\frac{1}{2}}[Pe]^{\frac{1}{2}}_{v,\max}. \tag{13a}$$

Both of these equations are plotted in Fig. 14 for a P/D ratio of 1·40.

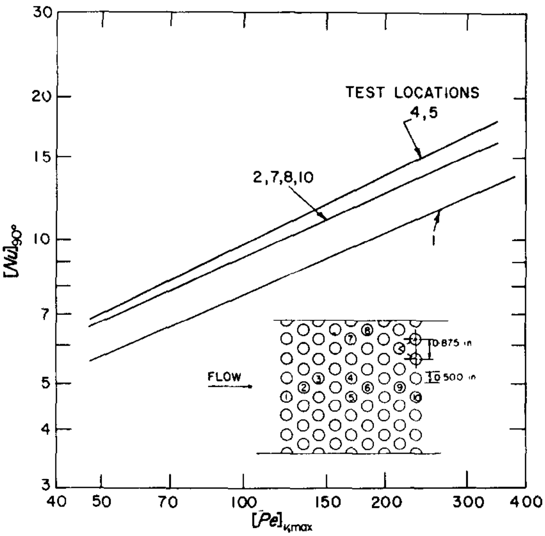

FIG. 7. Experimental heat-transfer results for 90° cross flow of NaK through a staggered rod bank, with only the test heated. Lines represent heat transfer characteristics for different rod locations in the bank.

4.2. *Experimental equipment and procedures*

The rod bank in the present study contains sixty-three rods including the unheated half-rods at the two side walls. They were arranged vertically in an equilateral pattern, as shown in Fig. 6, and the NaK flowed through them in a horizontal direction. All the rods were capable of being heated. Additional statistics on the test section are given in Table 1.

The basic design of the test elements, the methods of temperature and power measurements, and the experimental procedures were the same as those for the in-line-flow study.

For calculating both circumferentially local and rod-average heat-transfer coefficients, the bulk temperature was assumed to be the same as the inlet stream temperatures when only the test rod was heated. Under these conditions, the temperature rise of the NaK across the rod bank was always $<0{\cdot}3$°F. When all rods were heated, the method of determining the bulk temperature depended upon whether rod-average h's or local h's were being calculated. For the former, it was the bulk temperature calculated for the longitudinal position (in the bank) given by the center of the rod. For the latter, it was the bulk temperature calculated for the longitudinal position of the local point for which the h was being calculated.

In the series of runs in which all the rods were heated, cognizance was taken of the fact that the half-rods at the two side walls were not heated, in calculating the bulk temperature at a given location in the rod bank. It is assumed that the bulk temperatures at rod locations 1, 2, 3, 4, and 5 would be the same as if the half-rods were heated, i.e. it was assumed that rods in those locations would be "unaware" of the colder NaK flowing along at the sides. Data were not taken on a rod in location 8 because of the uncertainty in establishing the bulk temperature at that point, and data were not taken at location 6 because the rod in that location was a simple heating rod and not a test rod.

In the series of runs in which only the test rod was heated, data were not taken at locations 3, 6, and 9.

4.3. *Experimental results*

4.3.1. *When only test rod was heated.* Figure 6 shows the results obtained at test locations 4 and 5 in the interior of the lattice. It is seen that they agree very well with Hsu's [21] theoretical prediction based upon a simple cosine temperature distribution around the circumference of a rod. The precision of the data points is very good. They produce a straight line whose equation is

$$[Nu]_{90^\circ} = 0{\cdot}980\,[Pe]_{v,\,\max}^{0{\cdot}50} \tag{15}$$

which can be transformed to

$$[Nu]_{90^\circ} = 0{\cdot}923\,(\phi_1/D)^{0{\cdot}5}\left(\frac{P-D}{P}\right)^{0{\cdot}5}[Pe]_{v,\,\max}^{0{\cdot}5} \tag{15a}$$

by making use of the form of equation (12a). This equation is plotted in Fig. 9.

Figure 7 shows how the Nusselt number varied throughout the rod bank. The results are in good agreement with earlier results [4, 5] obtained at Brookhaven on mercury. The data points, omitted from the figure for the sake of clarity, had about the same precision as those shown in Fig. 6.

There have been considerable experimental data reported for the case of mercury flowing perpendicularly through staggered rod bundles. The conditions under which these data were taken are summarized in Table 3, and the results are presented graphically in

Table 3. Summary of experimental conditions under which lines in Fig. 8 were obtained

1. Investigators	Hoe *et al.* [4]	Rickard *et al.* [5]	Subbotin *et al.* [23]
2. Liquid metal	Hg	Hg	Hg
3. Surface metal	Cu	Cu, Cr	Ni
4. Rod cladding	Cu	Cu	Ni
5. Cladding thickness	0·049 in	0·049 in	2 mm
6. Wetting?	yes	yes/no	yes (?)
7. D	0·500 in	0·500 in	?
8. Pe range	330–1870	200–2000	100–5000
9. S_1/D	1·375	1·375	1·2
10. S_2/D	1·190	1·190	1·2, 1·3, 1·44, 1·5
11. Cold trap?	yes	yes	yes
12. Thermocouples imbedded in surface?	yes	yes	yes
13. No. of rods heated	test rod only	test rod only	1. test rod only 2. test rod and rods adjacent

Fig. 8. An average line drawn through these results would give the equation

$$[Nu]_{90^\circ} = 0{\cdot}633\,[Pe]_{v,\,\max}^{0{\cdot}56} \qquad (16)$$

and could be considered to represent quite well a P/D ratio of 1·40. Since $(\phi_1/D) = 3{\cdot}18$ for $(P/D) = 1{\cdot}40$, we can re-write the above equation as

$$[Nu]_{90^\circ} = 0{\cdot}644\,(\phi_1/D)^{\frac{1}{2}}\left(\frac{P-D}{P}\right)^{\frac{1}{2}}[Pe]_{v,\,\max}^{0{\cdot}56}. \qquad (16a)$$

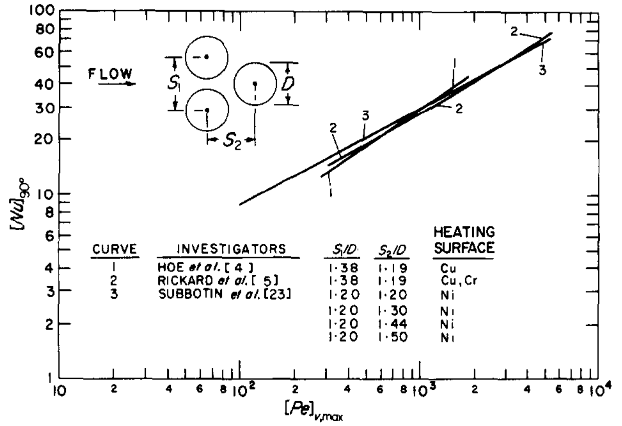

FIG. 8. Comparison of experimental results for 90°-cross flow of mercury through a staggered rod bundle, for a rod in the interior of the bundle, and for the case where only the test rod is transferring heat to the flowing stream.

For $P/D = 1{\cdot}75$, as in the present study, this equation can be reduced to

$$[Nu]_{90^\circ} = 0{\cdot}705\,[Pe]_{v,\,\max}^{0{\cdot}56}. \qquad (17)$$

Figure 9 compares this equation, based upon previous experimental results for mercury, with equation (15) which represents experimental results obtained in the present study. The agreement is excellent. There is no reason why there should be any difference between the two different liquid metals, as long as good wetting existed, and it should have existed in the three mercury studies and in the present one.

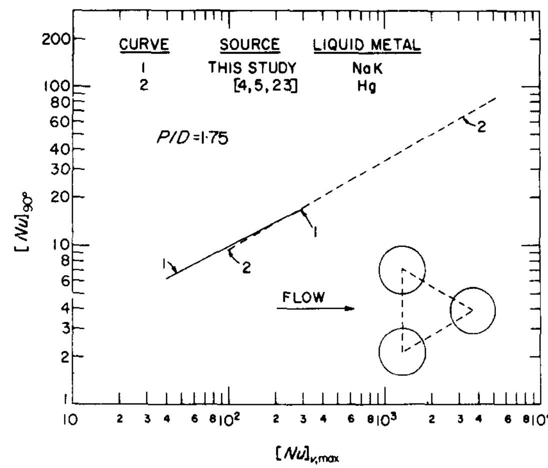

FIG. 9. Comparison of NaK and mercury heat-transfer results for 90°-cross flow through a staggered rod bank, for a rod in the interior of the bank, and for the condition of heat flux on the test rod only.

Because of the high shear and turbulence conditions in cross flow through rod bundles, the wetting of heat-transfer surfaces by alkali metals is apparently no problem.

4.3.2. *When all rods were heated.* The results for this part of the study are shown in Figs. 10 and 11. By comparing Figs. 7 and 10, it is seen that the curves in Fig. 10 are higher than those in Fig. 7. But it is also seen that the two sets tend to merge as the Péclet number (flow rate) is increased. By extrapolation, it is found that they actually merge at a Péclet number in the neighborhood of ≈600.

Although the present experimental study is presumably the only one to have been carried out with all the rods in the bank heated, Borishansky, Andreevsky, and Zhinkina [24] published results of an experimental study where the rods immediately surrounding the test rod were heated. Those authors used sodium, which had an oxygen content of 26 ppm; and their test bank contained three rods across and thirteen deep. Their test rod was located in the center of the bank, and it was constructed similarly to those used in the present study. In their paper, they did not specify the manner

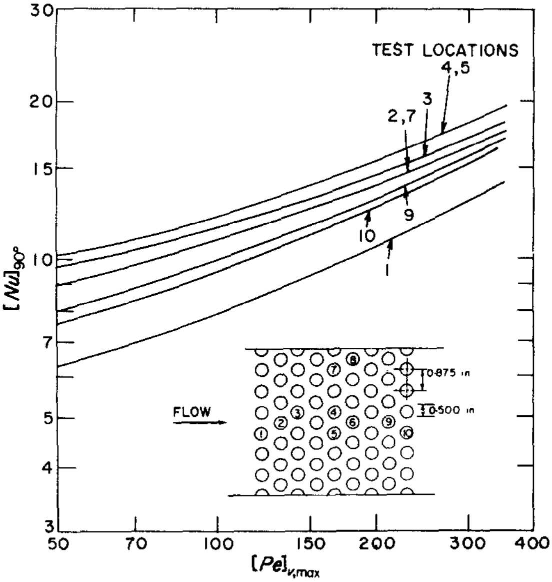

FIG. 10. Experimental heat-transfer results for 90°-cross flow of NaK through a staggered rod bank, with all rods heated. The various curves represent the heat-transfer characteristics for different rod locations in the bank.

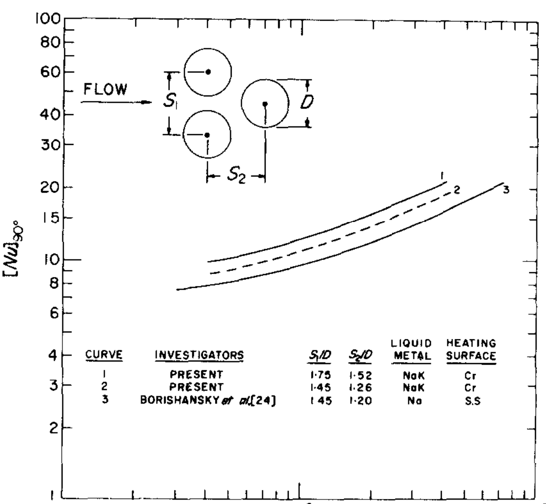

FIG. 11. Comparison of heat-transfer results for 90°-cross flow of liquid metals through staggered rod banks, for a rod in the interior of the bank. Curve 2 was obtained from 1 by making the necessary correction for change in P/D ratio, so that 2 and 3 could be on a comparable basis. Curve 1 was obtained for the condition where all the rods were heated, and 3 for the condition where the test rod and those immediately surrounding it were heated.

in which the bulk temperature was determined at the location of the test rod. The present authors do not see any clear-cut way of doing this when only the surrounding rods are heated.

Figure 11 gives a comparison between the results of Borishansky *et al.* and those obtained in the present study where all the rods were heated. Curve 1 is the same as the top curve in Fig. 10, and curve 2 was calculated from it. Curves 2 and 3 can be compared. The interesting thing is that, although curve 3 is about 12 per cent below 2, both curves are parallel. This contrasts sharply with the test-rod-heated-only curves which were straight.

The fact that curve 3 is appreciably lower than 2 is to be expected. There are two apparent reasons for this. First, due to the fact that the test bank of Borishansky *et al.* was only three rods wide, there would be a depressing side-wall effect. Curves 2 and 3 in Fig. 11 are entirely consistent with the top two curves in Figs. 7 and 10 where this effect is demonstrated. Secondly, the sheath of the test rod of Borishansky *et al.* was made of stainless steel, which has a low thermal conductivity compared to those of nickel and copper, the cladding materials used by the other investigators. Also, their test rod had a relatively large diameter. For these reasons, their thermal conditions were closer to those for uniform heat flux than to those for a simple cosine temperature distribution; which, as we can see by comparing equations (12a) and (13a), tend to make curve 3 fall below 2 in Fig. 11.

We can thus conclude that the results of the present study and those reported by Borishansky *et al.*, as compared in Fig. 11, are really in good agreement. The fact that different liquid metals are compared is inconsequential.

The question now is: "Why are test-rod-heated-only lines practically straight, while all-rods-heated lines are quite curved?" The present authors do not think that the curvature is due to the increasing importance of eddy conduction as the flow rate, and therefore the Péclet number increases. If this were true, the lines in Figs. 6

and 7 would not be straight either. In Fig. 8, although each line is straight, the three lines taken together suggest an "average" line with a slight upward curvature. There is considerable evidence that in the Péclet range shown in Fig. 11, eddy conduction is not a dominant mechanism in the heat-transfer process in cross flow.

The following question might well be asked: "Is the curvature due to the fact that the flow may be changing from laminar to turbulent?" In cross flow, this does not happen suddenly as the flow rate is increased; but rather it occurs over the $Dv_{max}\rho/\mu$ range of 10^2–10^3 [25]. A Reynolds number of 10^3 corresponds to a Péclet number of ≈ 20 for the NaK alloy used in the present investigation; and, since the minimum Péclet number for curve 2 in Fig. 11 is 40, the flow had to be fully turbulent. The same argument applies to curve 3.

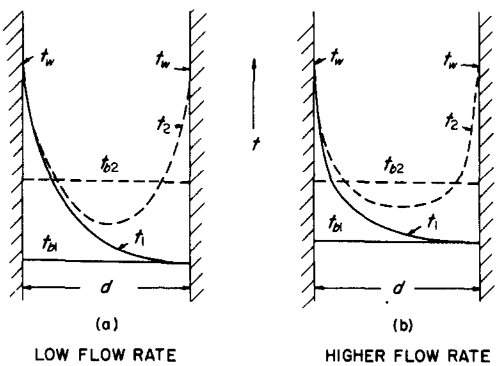

FIG. 12. Schematic drawings to illustrate why heating all rods yields higher coefficients than heating the test rod only. Wall temperatures and heat fluxes are the same in both cases. Subscript 1 refers to the case where only the test rod is heated, and 2 to the case where all the rods are heated. The dimension d represents the spacing between rods.

The present authors suggest that the curvature of the lines in Figs. 10 and 11 is explained by the temperature profiles in Fig. 12. Two sets of temperature profiles are shown. In Fig. 12(a), which represents a low flow rate, the profiles are less steep and the two bulk temperatures are farther apart than in Fig. 12(b), which represents a high flow rate. Thus, the coefficients in case (a) are farther apart than those in case (b); but, in both cases, the coefficients are greater when both walls are transferring heat.

From the three curves in Fig. 8 and from curve 2 in Fig. 11, it is possible to get a good estimate of a single curve covering the whole Péclet range, for the case where all the rods are heated, and for the case of $P/D = 1{\cdot}40$. The equation of this line is

$$[Nu]_{90^\circ} = 5{\cdot}90 + 0{\cdot}254\,[Pe]_{v,\,max}^{0{\cdot}635} \tag{18}$$

which, for any P/D ratio, becomes

$$[Nu]_{90^\circ} = \left(\frac{\phi_1}{D}\right)^{\frac{1}{2}}\left(\frac{P-D}{P}\right)^{\frac{1}{2}}\{6{\cdot}19 + 0{\cdot}2665\,[Pe]_{v,\,max}^{0{\cdot}635}\}. \tag{19}$$

Of course, this equation applies to the situation where we have a cosine temperature distribution around the circumference of the rod, which is generally the type of distribution one gets with copper sheaths, owing to the circumferential heat conduction. With thin stainless-steel sheaths, the thermal conditions should more closely approximate the case of uniform flux. For this condition, by analogy to equations (12) and (13), we can modify equation (19) and obtain the equation

$$[Nu]_{90^\circ} = \left(\frac{\phi_1}{D}\right)\left(\frac{P-D}{P}\right)^{\frac{1}{2}}\{5{\cdot}24 + 0{\cdot}225\,[Pe]_{v,\,max}^{0{\cdot}635}\}. \tag{20}$$

Equations (12a), (13a), (19), and (20) are all compared in Fig. 13 for a P/D ratio of 1·40. It is clear that in the intermediate Péclet range the theoretical equations agree very satisfactorily with the empirical ones. However, at the low and high ends of the Péclet range they predict low coefficients, particularly at the low end. At the low end, the coefficients are low because of assumption 7; at the high end, they are low because of assumption 2. It so happens that in the Péclet range normally encountered in commercial heat exchangers, test-rod-heated-only data are dependable for design purposes.

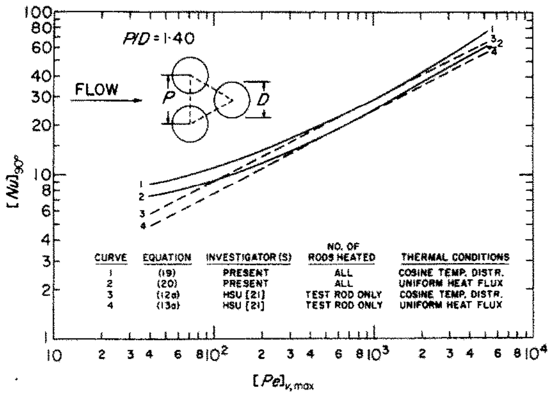

FIG. 13. Comparison of experimental heat-transfer results and theoretical predictions for 90°-cross flow of liquid metals through staggered rod banks, for a rod in the interior of the bank. Curves 1 and 2 represent experimental results obtained in this and previous studies [4, 5, 23].

4.3.3. *Local heat-transfer coefficients.* The design of the test rods used in the present study is explained in detail in [2]. Essentially they were special electrical-resistance heaters, consisting of a Nichrome coil embedded in magnesia electrical insulation and swaged in a copper tube. The O.D. of the rods was 0·500 in, and the thickness of the copper sheath was 0·100 in. Cooper was used for two reasons: first, it was easy to embed the surface thermocouples in it; and second, owing to its high thermal conductivity, the radial temperature gradient was small and therefore there would be a negligible error in the surface thermocouple readings due to slight radial variation in location.

Because the rod sheaths were quite thick and made of copper, there was appreciable circumferential heat flow through it. Hence the heat flux from a rod to the flowing NaK varied around the circumference. So, in order to determine local coefficients around the rod from the local surface temperatures, it was first necessary to estimate the local heat fluxes. This was done as follows [4].

The partial differential equation for steady-state heat conduction in the copper sheath with two dimensional heat flow is

$$\frac{\partial^2 t}{\partial r^2} + \frac{1}{r}\frac{\partial t}{\partial r} + \frac{1}{r^2}\frac{\partial^2 t}{\partial \theta^2} = 0. \tag{21}$$

The assumption is made that the heat flux at the inner wall of the copper sheath is uniform which gives us the first boundary condition, i.e.

$$\left.\frac{\partial t}{\partial r}\right)_{r=r_1} = \text{a constant} = c = -\frac{q)_{r=r_1}}{k_c} \tag{22}$$

It is found that the circumferential outer surface temperature variation can be expressed as a simple cosine function according to the experimental results of Hoe *et al.* [4], and as adopted by Hsu [21]. This gives us the second boundary condition, i.e.

$$t_{w,\theta} - t_{w,0°} = a(1 - \cos\theta). \tag{23}$$

In some cases, it was found that when a equalled

$$t_{w,90°} - t_{w,0°} \tag{24}$$

a very good fit of equation (23) to the measured temperature profiles was obtained. In most cases, however, it was necessary to change slightly the value of a to give a good fit in the narrow region around the rear stagnation point.

Equations (21–23) were solved to give $t = f(r, \theta)$. This was then differentiated to give $\partial t/\partial r = f(r, \theta)$, from which $\partial t/\partial r)_{r=r_2} = f(\theta)$ was obtained. Finally, h for any value of θ was obtained from the heat-balance equation

$$h_\theta(t_{w,\theta} - t_b) = -k_c\left(\frac{\partial t}{\partial r}\right)_{r=r_2}. \tag{25}$$

It was found that the circumferential variation of h was the same whether all rods in the test section were heated or whether only the particular test rod was heated. It was further found that the relative variation of h_θ, i.e. $h_\theta/\bar{h}_{w,90°}$ or $h_\theta/h_{0°}$, around the circumference was almost independent of Péclet number (flow rate). These observations confirm the validity of assumptions 2 and 7, respectively. It was also confirmed that

$$h_{90°} = \bar{h}_{w,90°}. \tag{26}$$

The experimental results are shown graphically in Figs. 14 and 15. The data points are not plotted; their average deviation from the lines shown were only about ± 1 per cent. It is seen in Fig. 15 that the coefficients at the rear stagnation point, for all test conditions, are just one-fifth those at the forward stagnation point.

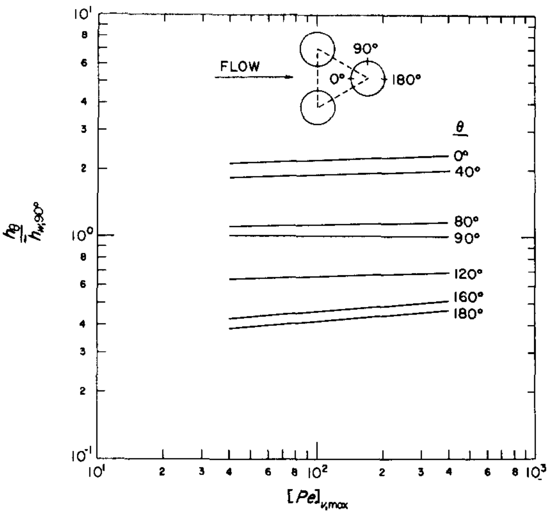

FIG. 14. Experimental heat-transfer results for 90°-cross flow of NaK through a staggered rod bank showing the circumferential variation of the local heat-transfer coefficient.

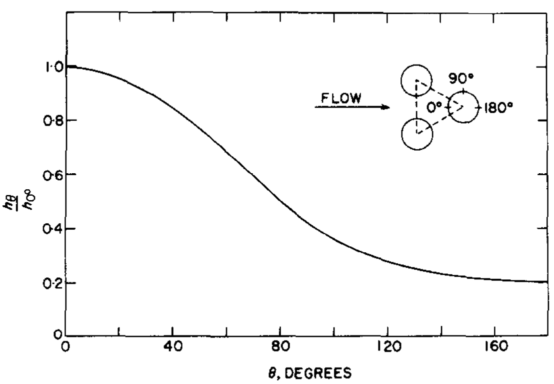

FIG. 15. Experimental heat-transfer results for 90°-cross flow of NaK through a staggered rod bank showing the circumferential variation of the local heat-transfer coefficient.

If we ignore the slight variation of the ratio $h_\theta/\bar{h}_{w,90°}$ with Péclet number, we can express it by the empirical equation

$$h_\theta/\bar{h}_{w,90°} = 1 - 1{\cdot}22\cos(180 - \theta) \tag{27}$$

for $0° \leqslant \theta \leqslant 90°$, and by the equation

$$h_\theta/\bar{h}_{w,90°} = 1 - 0{\cdot}58\cos(180 - \theta) \tag{28}$$

for $90° \leqslant \theta \leqslant 180°$, where $\bar{h}_{w,90°}$ is calculated from equation (15a) when only the test rod is heated, and from equation (19) where all the rods are heated. With these equations, the circumferential variation of the surface temperature is readily calculated for a given set of experimental conditions encompassed by the present study.

Referring to Fig. 14 again, the reader is reminded that $\bar{h}_{w,90°}$ is not h_θ averaged over the circumference of a rod. It is based upon the average surface temperature and the average heat flux.

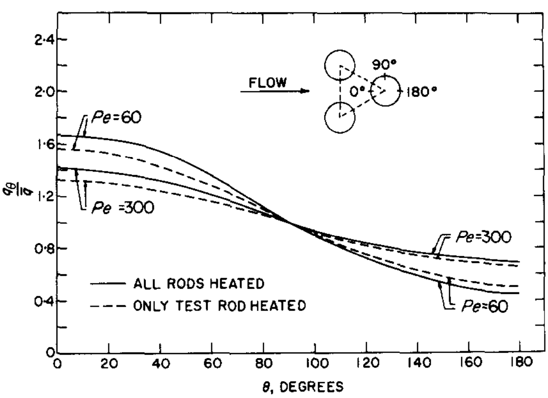

FIG. 16. Circumferential variation of the local heat flux obtained in the present study, for 90°-cross flow, and for a rod in the interior of the bank.

Figure 16 shows the circumferential variation of the local heat flux for the conditions of the present experiments. There is a slight effect of flow rate, and in the direction one would expect.

5. 45°-CROSS FLOW

5.1. *Theoretical considerations*

Hsu extended his analytical study of 90° cross flow [21] through staggered rod bundles, or banks, to the general case of oblique flow [26]. In the latter study, he made all the same assumptions he had made in the former and one additional one. This additional one was that heat-transfer coefficients for oblique flow are the same as 90°-cross flow through a bank of elliptical rods. The shape of the elliptical cross-section is determined by an imaginary plane cutting across a circular rod in such a way that a second plane passing through the axis of the rod intersects the first plane at right angles and defines a straight line which is parallel to the direction of flow through the bank.

In deriving average heat-transfer coefficients for elliptical rods located in the interior of a bank, Hsu assumed that the distribution of hydrodynamic potential around the surface of a rod could be expressed by a cosine function in terms of elliptical coordinates. He also assumed that the circumferential temperature distribution around an elliptical rod was that of a simple cosine function when the ellipse was transformed to a circle, which was consistent with his analysis for 90°-cross flow through a bank consisting of circular rods. For this case, his final equation was

$$[Nu]_\beta = 1{\cdot}064\left(\frac{\phi_1}{a+b}\right)^{\frac{1}{2}}[Pe]^{\frac{1}{2}}_{v,\,\mathrm{free}} \times \frac{[(1-e^2)+(1-e^2)^{\frac{1}{2}}]^{\frac{1}{2}}}{E} \tag{29}$$

where a and b represent the major and minor axes, respectively, of the ellipse; $[Pe]_{v,\,\mathrm{free}}$ is based upon the velocity which the liquid metal would have if the rods were absent from the shell; $e = (a^2 - b^2)^{\frac{1}{2}}/a$ = eccentricity of the ellipse; and E = the complete elliptical integral of the second kind, defined by

$$\int_0^{\pi/2} (1 - e^2 \sin^2 \lambda)^{\frac{1}{2}}\, \mathrm{d}\lambda. \tag{30}$$

Hsu has given values of $\phi_1/(a + b)$ in graphical form for both triangular and square arrays. It so happens that the relationship between $\phi/(a + b)$ and $(a + b)/P$ is the same as that between ϕ_1/D and D/P for perpendicular flow across circular rods.

Theoretically, equation (29) covers all flow directions from perpendicular to parallel. However, owing to the basic assumption made in its derivation, which was mentioned above, it is less reliable as the angle of flow, β, approaches zero, i.e. parallel flow. For the range $10° \leqslant \beta \leqslant 90°$, Hsu [27] has proposed a reliable modification of this equation. It is

$$[Nu]_\beta = 0{\cdot}958\,(\phi_1/D)^2\,[Pe]^{\frac{1}{2}}_{v,\,\mathrm{free}} \times \left[\frac{(1-e^2)+(1-e^2)^{\frac{1}{2}}}{2-e^2}\right]^{\frac{1}{2}} \tag{31}$$

which is equation (12), for 90°-cross flow, multiplied by the eccentricity term in the square brackets. Dwyer [19] further modified this equation to the more convenient form

$$[Nu]_\beta = 0{\cdot}958\,(\phi_1/D)^{\frac{1}{2}}\left(\frac{P-D}{P}\right)^{\frac{1}{2}}[Pe]^{\frac{1}{2}}_{v,\max} \times \left[\frac{\sin\beta + \sin^2\beta}{1+\sin^2\beta}\right]^{\frac{1}{2}}. \tag{32}$$

In this equation, ϕ_1/D is evaluated from the curve in Fig. 17, as in the case of 90°-cross flow, and P and D refer to the actual pitch and diameter of the rods.

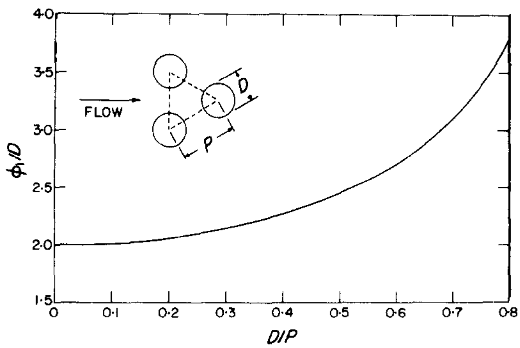

FIG. 17. Dependence of the normalized hydrodynamic potential drop, ϕ_1/D, on the D/P ratio, for perpendicular flow through rod bundles or tube banks having an equilateral triangular spatial arrangement (from Hsu [21]).

For the case of uniform heat flux, from equation (13a) it is seen that the coefficient in equations (31) and (32) should be changed to 0·810.

5.2. *Experimental equipment and prøcedures*

These were very much the same as for the 90°-cross-flow study. The rod size, number, and spacing were the same. The distance between the top and bottom plates of the rectangular shell was also the same. The only difference was that the rods were inclined at a 45° angle with respect to the horizontal. A schematic side view of the test section is shown in Fig. 18.

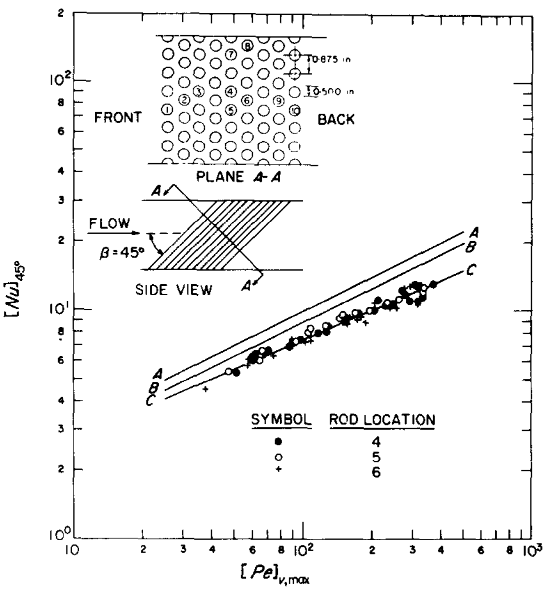

FIG. 18. Nusselt numbers for 45°-cross flow of liquid metals through a staggered rod bank, for rods in the interior of the bank, and for the test rod only transferring heat. The data points and line C–C represent experimental results obtained in the present study with NaK, while lines A–A and B–B represent theoretical equations (29) and (32) proposed by Hsu [26, 27].

Data were not taken at rod locations 3, 7, 8, and 9. Further information on the design of the 45°-cross-flow test section, as well as on the scope of this portion of the work, is given in Table 1.

5.3. *Experimental results*

5.3.1 *When only the test rod was heated.* The bulk temperatures on which the calculated heat-transfer coefficients are based were defined in the same manner as those for the 90°-cross-flow coefficients.

The rod-average heat-transfer coefficients, in terms of Nusselt numbers, are shown in Figs. 18 and 19. In Fig. 18 lines A–A and B–B represent equations (29) and (32), respectively—the theoretical equations by Hsu.

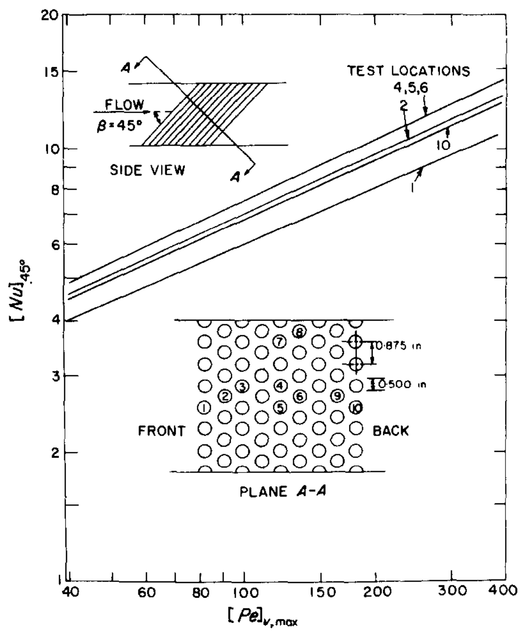

FIG. 19. Experimental heat-transfer results for 45°-cross flow of NaK through a staggered rod bank, with only the test rod heated. Lines represent heat-transfer characteristics for different rod locations in the bank.

Line A–A falls 25–40 per cent above C–C; and line B–B, 15–25 per cent. It is seen in Section 4.3.1 that equation (12a), which is the same as equation (32) for 90°-cross flow, agreed very well with the 90°-cross-flow results; and therefore, since the accuracy of the 45°-cross-flow results should be just as high as those, the only conclusion is that both equations (29) and (32) are not reliable for values of β far from 90°.

The apparent reason for this is the assumption (made in their derivations) that oblique flow across a circular rod is the same as perpendicular flow across an elliptical rod, as far as convective heat is concerned. It is obvious that this is not so at the limit where $\beta \to 0$. In that case, Hsu's model reduces to the case of flow past a flat plate rather than in-line flow through a bundle of rods.

Line C–C in Fig. 18 represents the equation

$$[Nu]_{45°} = 1{\cdot}014\,[Pe]_{v,\,\max}^{0{\cdot}432}. \tag{33}$$

Thus, its slope is lower than that observed for 90°-cross flow as well as the theoretically predicted value, both of which are 0·5. This does not necessarily mean that the experimental results in Fig. 18 are probably less accurate. The slope of 0·5 in the 40–400 Péclet range is not sacrosanct, as we saw earlier.

On the basis of the present results, however, it is possible to write the equation

$$[Nu]_{\beta} = 0{\cdot}84\,[Nu]_{90°}\left[\frac{\sin\beta + \sin^2\beta}{1 + \sin^2\beta}\right]^{\frac{1}{2}} \tag{34}$$

as a close approximation for: oblique flow, a rod in the interior of a bank, test rod heated only, $40 \leqslant Pe)_{v.\,\max} < 400$, and $30° \lesssim \beta \leqslant 90°$. This equation says that as β goes from 90° to 45°, the rod-average heat-transfer coefficient decreases about 25 per cent; and from 90° to 30°, 35 per cent. These are large reductions. Figure 19 has a family of lines showing the effect of rod location (in the bank) on the average heat-transfer coefficient (expressed as Nusselt numbers). The lines fall pretty much as would be expected on the basis of the results for the 90°-cross-flow case shown in Fig. 7.

5.3.2. *When all the rods were heated.* The results for this case turned out to be unsatisfactory. The measured temperature rise of the NaK flowing through the test section was greater than that obtainable if there were no heat losses; which, in the 90°-cross-flow studies, fell in the range of 1–5 per cent, depending upon the flow rate. This led us to suspect that there was inadequate mixing in the bank, and that temperature striations in the NaK stream were giving us our erroneous exit temperature readings. This was confirmed when temperature data were taken with only the first three rows of rods heated. Under those conditions, the succeeding six rows thoroughly mixed the stream, and the exit temperature readings indicated heat losses in the proper range, i.e. 1–5 per cent.

By referring to the diagram in Fig. 20, it is seen that the path of least resistance to flow, for the colder fluid at the top, is not straight through the bank, but along the shorter, diagonal path. This means that there is a faster moving, and therefore colder, stream flowing in the diagonal direction, as indicated. This would further mean that the middle portion of a rod in the center of the bank would run colder than either of its end portions. As a result, the central rod would tend to give higher coefficients since the surface temperatures were measured at the mid-points of the rods (point b in the figure). By this argument, element 10 (point c in the figure) should have given low coefficients because its thermocouples would be in a relatively hotter region; and it actually did. The coefficients of test element 1 (point a in the figure) were, as one would expect, little different from those obtained on it when it was the only rod heated.

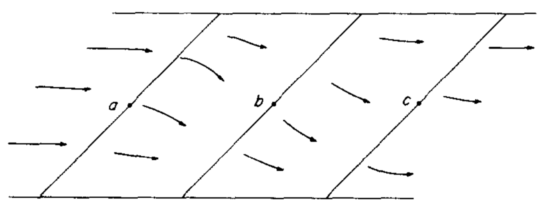

FIG. 20. Schematic drawing to illustrate short-circuiting of flow through 45°-rod bank.

It is therefore apparent that the coefficients could be off for two reasons: measured wall temperatures which were too low, and erroneous bulk temperatures. It must be remembered that only 2 deg or 3 degF difference in $(\bar{t}_{w,45°} - t_b)$ could account for the discrepancy.

Rod-averaged coefficients calculated by all plausible ways for rod locations 4, 5, and 6 came significantly higher, relative to the test-rod-heated-only coefficients, than did those for the 90°-cross-flow case. However, they did merge with the test-rod-heated-only line (presented in Figs. 18 and 19) at $Pe \approx 600$, showing that if the turbulence was increased enough, the temperature striations disappeared.

On the basis of the results presented above and by making use of the results shown graphically in Fig. 13, the following empirical equation is recommended for estimating oblique-flow coefficients for a rod in the interior of a bank when all rods in the bank are heated, when the circumferential surface temperature variation approximates that of a simple cosine, and when $30° \gtrsim \beta \leqslant 90°$.

$$[Nu]_\beta = (\phi_1/D)^{\frac{1}{2}}\left(\frac{P-D}{P}\right)^{\frac{1}{2}}\left[\frac{\sin\beta+\sin^2\beta}{1+\sin^2\beta}\right]^{\frac{1}{2}} \times \left[5{\cdot}44 + 0{\cdot}228\,[Pe]^{0{\cdot}614}_{v,\,\max}\right]. \quad (35)$$

For the case of uniform heat flux, the last square-bracketed term should be changed to

$$4{\cdot}60 + 0{\cdot}193\,[Pe]^{0{\cdot}614}_{v,\,\max}. \quad (36)$$

5.3.3 *Local heat-transfer coefficients.* Each test rod had its nine surface thermocouples located at the same axial distance along the rod, i.e. they were located in the rod's diametral circle, not in the circumference of the imaginary ellipse.

It was found that the circumferential surface temperature variations, like those for the 90°-cross-flow case, represented a simple cosine distribution. This is confirmation of one of Hsu's [26] assumptions in his theoretical analysis.

It was found that the circumferential variations of the local coefficients for the 45°-cross-flow case were identical with those for the 90°-cross-flow case, at least for the situation where only the test rod was heated. Local coefficients were not calculated for the all-rods-heated situation because of the experimental difficulties described in the previous section. Thus, the curves in Figs. 14 and 15 are also applicable to the 45°-cross-flow situation.

ACKNOWLEDGEMENTS

The authors gratefully acknowledge the assistance of the many members of the Nuclear Engineering Department at Brookhaven who helped to carry out this study. Special thanks are due to K. C. Hoffman and S. J. Majeski for their help in the design of the loop; C. Scarlett for supervising its construction; and A. Kokinelis and W. J. Lewis, Jr. for assisting materially in its operation.

REFERENCES

1. A. J. FRIEDLAND, O. E. DWYER, M. W. MARESCA and C. F. BONILLA, Heat transfer to mercury in parallel flow through bundles of circular rods, in *Proceedings of the Second International Heat Transfer Conference*, Boulder, Colo. Am. Inst. Chem. Engrs, New York (1961).
2. M. W. MARESCA and O. E. DWYER, Heat transfer to mercury flowing in-line through a bundle of circular rods, *J. Heat Transfer* **86**, 180–186 (1964).
3. B. NIMMO and O. E. DWYER, Heat transfer to mercury flowing in-line through a rod bundle, *J. Heat Transfer* **87**, 312–313 (1965).
4. R. J. HOE, D. DROPKIN and O. E. DWYER, Heat transfer rates to cross-flowing mercury in a staggered tube bank–I, *Trans. Am. Soc. Mech. Engrs* **79**, 899–907 (1957).
5. C. L. RICKARD, O. E. DWYER and D. DROPKIN, Heat transfer rates to cross-flowing mercury in a staggered tube bank—II, *Trans. Am. Soc. Mech. Engrs* **80**, 642–652 (1958).
6. Quarterly Status Report on Advanced Reactor Technology (ART), for period ending October 31, 1966. USAEC Report LA-3625-MS, p. 12, Los Alamos Scientific Laboratory of the University of California (November 1966).
7. *Liquid Metals Handbook, Sodium–NaK Supplement*, edited by C. B. JACKSON. Atomic Energy Commission and Department of the Navy, Washington, D.C. (1955).
8. O. E. DWYER and P. S. TU, Analytical study of heat-transfer rates for parallel flow of liquid metals through tube bundles, Part I, *Chem. Engng Prog. Symp. Ser.* **56**, 183–193 (1960).
9. A. J. FRIEDLAND and C. F. BONILLA, Analytical study of heat-transfer rates for parallel flow of liquid metals through tube bundles, Part II, *A.I.Ch.E. Jl* **7**, 107–112 (1961).
10. V. S. OSMACHKIN, Some problems of heat transfer in liquid-cooled reactors, in *Proceedings of the Third UN International Conference on the Peaceful Uses of Atomic Energy*, Geneva, Vol. 8, pp. 128–139 (September 1964).
11. O. E. DWYER, Analytical study of heat transfer to liquid metals flowing in-line through closely packed rod bundles, *Nucl. Sci. Engng* **25**, 343–358 (1966).
12. O. E. DWYER, Eddy transport in liquid-metal heat transfer, *A.I.Ch.E. Jl* **9**, 261–268 (1963).

13. N. A. AMPLEEV, P. L. KIRILLOV, V. I. SUBBOTIN and M. Y. SUVOROV, Liquid-metal heat exchange in a vertical tube at low values of the Péclet number, State Committee on the Use of Atomic Energy, USSR (1965).
14. V. I. SUBBOTIN, M. K. IBRAGIMOV and E. V. NOMOFILOV, Heat transfer in a region of thermal stabilization in the turbulent flow of liquid metals in a tube, *Atom. Energy* **13**, 155–161 (1962).
15. V. I. SUBBOTIN, M. K. IBRAGIMOV, N. V. IVANOVSKY, M. N. AROL'DOV and E. V. NOMOFILOV, Turbulent heat transfer in a flow of liquid metals, *Int. J. Heat Mass Transfer* **4**, 79–87 (1961).
16. V. I. SUBBOTIN, P. A. USHAKOB and P. L. KIRILLOV. Heat removal from reactor fuel elements cooled by liquid metals, in *Proceedings of the Third UN International Conference on the Peaceful Uses of Atomic Energy*, Geneva, Paper No. 328 (September 1964).
17. V. M. BORISHANSKY and G. V. FIRSOVA, Heat exchange in longitudinal flow of metallic sodium past a tube bank, *Atom. Energy* **14**, 584–585 (1963).
18. V. M. BORISHANSKY and E. V. FIRSOVA, Heat exchange in separated bundles of rods with metallic sodium flowing longitudinally, *Atom. Energy* **16**, 457 (1964).
19. O. E. DWYER, Recent developments in liquid-metal heat transfer, *Atom. Energy Rev.* **4**, 3–92 (1966).
20. R. D. CESS and R. J. GROSH, Heat transmission to fluids with low Prandtl numbers for flow through tube banks, *Trans. Am. Soc. Mech. Engrs* **80**, 677 (1958).
21. C. J. HSU, Analytical study of heat transfer to liquid metals in cross flow through rod bundles, *Int. J. Heat Mass Transfer* **7**, 431 (1964).
22. R. C. J. HOWLAND and B. W. MCMULLEN, Potential functions related to groups of circular cylinders, *Trans. Camb. Phil. Soc.* **32**, 402 (1936).
23. V. I. SUBBOTIN, V. E. MINASHIN and E. I. DENISKIN, Heat exchange in flow across tube banks, *Teplofiz. Vysok. Temp.* **1**, 238 (1963).
24. V. M. BORISHANSKY, A. A. ANDREEVSKY and V. B. ZHINKA, Heat transfer to cross-flowing sodium in a staggered tube bank, *Atom. Energy* **13**, 269–271 (1962).
25. O. P. BERGELIN, G. A. BROWN and S. C. DOBERSTEIN, Heat transfer and fluid friction during flow across banks of tubes, *Trans. Am. Soc. Mech. Engrs* **74**, 953–959 (1952).
26. C. J. HSU, Heat transfer to liquid metals flowing past spheres and elliptical rod bundles, *Int. J. Heat Mass Transfer* **8**, 303–315 (1965).
27. C. J. HSU. Brookhaven National Laboratory, Upton, N.Y., Private communication (January 1966).

Résumé—On présente les résultats d'une étude expérimentale complète sur la chaleur apportée à du Nak s'écoulant à travers des faisceaux (ou rangées) de barreaux sans écrans.

Les résultats de l'écoulement longitudinal sont donnés sur neuf barreaux essayés différents situés au centre d'une faisceau de 19 barreaux. Ils ont été obtenus avec des profils de vitesse et de température entièrement établis et aussi dans le cas de la région d'entrée. Les résultats pour les cinq premiers barreaux essayés étaient en très bon accord avec les prévisions théoriques et avec les résultats précédents sur le mercure; mais, ceux sur les quatre derniers barreaux sont entièrement dans le régime de conduction moléculaire (faibles nombres de Péclet). Plus la vitesse d'écoulement est faible, plus les coefficients diminuent, ce qui indiquent la présence d'une résistance interfaciale qui est très sensible à la vitesse de l'écoulement. On en a conclu que la difficulté provenait du mouillage médiocre de la surface chauffante. La concentration d'oxygène dans le Nak était constamment égale à 25 ppm, ce qui est loin au-dessous du niveau de saturation correspondant à la partie la plus froide de la boucle de circulation.

Des résultats ont été également obtenus pour des écoulements perpendiculaires et à 45° à travers les faisceaux de barreaux, dans le cas où seul le barreau essayé était chauffé et dans le cas où tous les barreaux l'étaient. On a effectué des mesures pour des barreaux placés à divers endroits dans le groupe, et on a obtenu les coefficients de transport de chaleur en chaque point de la circonférence et les coefficients moyens.

Les résultats de l'écoulement perpendiculaire étaient en bon accord avec des résultats publiés précédemment sur le mercure, et avec les prévisions basées sur la corrélation théorique de Hsu [21]. Dans la région des faibles nombres de Péclet, les coefficients dans le cas où tous les barreaux sont chauffés étaient beaucop plus élevés que ceux dans le cas où seul le barreau essayé était chauffé, mais la différence diminuait lorsque la vitesse de l'écoulement augmentait.

Les coefficients pour l'écoulement à 45°, plus faibles que les prévisions théoriques de Hsu [26, 27] étaient égaux à 75% de ceux pour le cas de l'écoulement à 90°.

La variation en fonction de l'azimuth du coefficient de transport de chaleur normalisé est indépendante de la vitesse de l'écoulement pour les deux directions de l'écoulement à 90°. La variation de la température de surface le long de la circonférence était celui d'une simple fonction en cosinus, pour les deux types d'écoulement.

Sur la base des résultats obtenus dans cette étude, confirmés par des résultats théoriques et expérimentaux antérieurs, on propose des équations semi-empiriques pour prédire les coefficients de transport de chaleur pour les écoulements à 90 et à 45°, dans le cas où seul le barreau essayé est chauffé et dans celui où tous les barreaux sont chauffés.

Zusammenfassung—Der Bericht vermittelt die Ergebnisse einer umfangreichen experimentellen Untersuchung über den Wärmeübergang an NaK, das durch Stabbündel ohne Einbauten strömt. Es werden Ergebnisse wiedergegeben für neun verschiedene Versuchsstäbe, die in der Mitte eines Bündels aus 19 Stäben angeordnet sind und axial angeströmt werden. Die Versuche wurden sowohl bei abgeschlossenem hydrodynamischen une thermischen Einlauf, als auch im Einlaufsbereich durchgeführt. Die Ergebnisse der ersten 5 Versuchsstäbe sind in brauchbarer Übereinstimmung mit theoretischen Voraussagen und früheren Versuchen, die mit Quecksilber durchgeführt wurden. Die Ergebnisse für die letzten 4 Stäbe liegen jedoch unterhalb des Gebiets der molekularen Wärmeleitung (kleine Pecletzahl). Je geringer die Massenstromdichte wird, desto geringer werden auch die Wärmeübergangszahlen. Dies deutet auf einen Widerstand an der Kontaktfläche hin, der sich stark mit der Massenstromdichte ändert. Dieser Unstand wird auf eine unvollkommene Benetzung der wärmeabgebenden Fläche und auf die Anwesenheit von Schutzgas an dieser Fläche zurückgeführt. Die Sauerstoffkonzentration in NaK war zu jeder Zeit kleiner als 25 ppm. Das ist weit weniger, als die der kältesten Stelle des Kreislaufs entsprechende Sättigungskonzentration.

Bei den Versuchen mit querangeströmten (90°) und schräg angeströmten (45°) Stabbündeln wurde entweder nur der Versuchsstab oder alle Stäbe beheizt. Die Messungen wurden bei verschiedenen Stabpositionen gemacht. Sowohl die mittleren Wärmeübergangszahlen am Stab, als auch die lokalen Wärneübergangszahlen am Umfang wurden ermittelt.

Die Ergebnisse der Versuche bei senkrechter Anströmung sind in guter Übereinstimmung mit früher veröffentlichten Ergebnissen mit Quecksilber und mit Berechnungen nach der theoretischen Beziehung von Hsu [21]. Werden alle Stäbe beheizt, so liegen die Wärmeübergangszahlen im Gebiet kleiner Pecletzahlen merklich höher also bei der Beheizung nur eines Versuchsstabes. Diese Differenz wird kleiner mit grösser werdender Massenstromdichte.

Die Wärmeübergangszahlen bei schräger Anströmung unter 45°, die niedriger liegen als die theoretischen Vorhersagen von Hsu [26, 27], betragen 75% der Werte bei 90° Queranströmung.

Die Änderungen der örtlichen, bezogenen Wärmeübergangszahlen in Umfangsrichtung sind unabhängig von der Massenstromdichte und sind die gleichen bei 45° und 90° Anströmrichtung. Bei beiden Anströmrichtungen ist der Verlauf der Oberflächentemperatur in Umfangsrichtung der einer einfachen Kosinusfunktion.

Auf der Grundlage dieser Ergebnisse und mit Hilfe früherer theoretischer und experimenteller Aussagen werden halb-empirische Gleichungen angegeben. Mit ihrer Hilfe kann man die Wärmeübergangskoeffizienten für 90° und 45° Anströmrichtung berechnen, sei es für den Fall, dass nur der Versuchsstab beheizt wird, oder für den Fall, dass alle Stäbe beheizt sind.

Аннотация—В статье приводятся результаты обширного экспериментального исследования переноса тепла к NaK, текущему через пучки труб без перегородок.

Сообщаются данные опытов для параллельного расположения стержней, полученные на девяти различных стержнях, помещенных поодиночке в центре пучка из девятнадцати стержней. Опыты проводились при полностью установившихся профилях скорости и температуры, а также во входной области. Результаты для первых пяти стержней хорошо согласуются с теоретическими расчетами, а также с ранее полученными данными для ртути; но результаты для последних четырех стержней относятся к режиму низкой молекулярной теплопроводности (малые числа Пекле). Чем ниже скорость движения, тем меньше коэффициенты. Этот факт указывает на наличие сопротивления на границе раздела фаз, весьма чувствительного к скорости течения. Можно заключить, что трудность вызвана неидеальным смачиванием поверхности нагрева. Концентрация кислорода в NaK составляла 25 частей на миллион в каждом случае, что много ниже уровня насыщения, соответствующего самой холодной циркуляционной петли.

Также получены результаты для поперечнообтекаемых (90°) и кособтекаемых (45°) пучков стержней при условии нагрева только одного исследуемого стержня или одновременного нагрева всех стержней. Проводились измерения для нескольких расположений стержней в пучке; получены усредненные и локальные коэффициенты теплообмена.

Результаты для поперечнообтекаемых пучков хорошо согласуются с ранее опубликованными данными для ртути и с расчетами, основанными на теоретическом соотношении Хсу [21]. При малых числах Пекле и одновременном нагреве стержней коэффициенты оказываются значительно выше, чем для случая нагрева только одного стержня, и эта разница уменьшается с увеличением скорости потока.

Коэффициенты для кособтекаемых пучков оказываются ниже коэффициентов, найденных теоретически Хсу [26, 27], и составляют 75% от коэффициентов для случая поперечного обтекания.

Найдено, что азимутальное изменение локального нормализованного коэффициента теплообмена не зависит от скорости для исследованных расположений пучка по отношению к вектору скорости набегающего потока. Для обоих типов течений температурное распределение на поверхности имеет вид синусоидальной функции.

На основе полученных результатов, подтвержденных теоретическими и экспериментальными данными, предлагаются полуэмпирические уравнения для оценки коэффициентов теплообмена поперечно — и кособтекаемых пучков в случае нагрева только одного стержня или всех стержней одновременно.